Final version published as: "Colloidal Core-Shell Materials with 'Spiky' Surfaces Assembled from Gold Nanorods," Guo, I.W.; Pekcevik, I.C.; Wang, M.C.P.; Kinkead, B.; Gates, B.D., Chem. Commun., 2014, 50 (60), 8157-8160. DOI: 10.1039/c4cc02410a.

Colloidal Core-Shell Materials with 'Spiky' Surfaces Assembled from Gold Nanorods

Iris W. Guo,[a] Idah C. Pekcevik,[a] Michael C.P. Wang,[a] Brandy K. Pilapil,[a] and Byron D. Gates[a,*]

A series of core-shell materials with 'spiky' surfaces are prepared through the self-assembly of gold nanorods onto polystyrene microspheres. Loading of the nanorods is finely tuned and the assemblies exhibit surface plasmon resonance properties. The 'spiky' surface topography of the assembled structures could serve as a versatile substrate for surface enhanced Raman spectroscopy based sensing applications.

A new class of colloidal core-shell materials are prepared with multiple 'spikes' formed from the self-assembly of gold nanorods (AuNRs) onto a spherical polystyrene (PS) core. These assemblies are systematically prepared and analysed for their colloidal and optical properties. These and other core-shell materials form an interesting type of particles where the core serves as a platform to guide the growth or assembly of a shell layer.[1,2] This outer shell layer is often sought for the new properties it imparts onto the underlying core material, such as magnetization,[3,4] localized surface plasmon resonance (LSPR),[3,5] fluorescence emission,[6,7] catalytic reactivity,[8,9] and a distinct surface chemistry.[10,11] These core-shell materials can also serve as a template for the development of other functional materials.[11-13] The preparation of assemblies of gold nanoparticles on the polystyrene core can also be sought to retain the properties of individual nanoparticles,[14] rather than transitioning to those of a bulk-like material.

There exists a diverse range of procedures to form core-shell particles composed of discrete gold nanoparticles on a spherical template. In some of these approaches, spherical gold nanoparticles are first synthesized and subsequently assembled onto either a silica or PS core.[15-19] Citrate capped spherical gold nanoparticles have been assembled onto amine-functionalized silica cores through electrostatic interactions.[15-17] In these assemblies, the loading of spherical gold nanoparticles could be tuned from a sub-monolayer to a complete shell.[16] Previous studies have also demonstrated the possibility of preparing core-shell assemblies of AuNRs on a silica core.[16] Another approach to achieve core-shell materials with a shell of discrete gold nanoparticles is to directly synthesize the nanoparticles onto the core.[14,20-22] Spherical gold nanoparticles can be grown on the surfaces of amine-functionalized silica cores[20] or sulfonate-functionalized PS spheres.[22] A modification of this approach is to nucleate the gold nanoparticles in the presence of PS spheres and to form the core-shell assemblies through a process of heterocoagulation.[14] Assemblies of AuNRs on silica cores have also been directly prepared through growth of the AuNRs within a polyelectrolyte multilayer encapsulating the silica core.[21] We introduce the formation of core-shell assemblies with tuneable loadings of AuNRs on a spherical PS core (PS@AuNRs) with a corresponding transition in surface topography (Fig. 1). The orientation of the AuNRs relative to the PS core changes at high loadings, creating a roughened or 'spiky' surface topography containing multiple AuNRs. The plasmonic characteristics of the assemblies and also their increased the surface roughness could be useful in sensing applications including surface-enhanced Raman spectroscopy (SERS).[23-26] The SERS properties of these assemblies are compared as a function of the different surface topographies observed for relatively low and high loadings of AuNRs.

We systematically prepared a series of PS@AuNRs assemblies through the dispersion of polyvinylpyrrolidone (PVP) and sodium dodecyl sulfate (SDS) capped AuNRs[27] under acidic conditions in ethanol based solutions containing amine-functionalized PS spheres. These PVP and SDS stabilized AuNRs adhere to the surfaces of the PS spheres during the formation of the PS@AuNRs assemblies (Fig. 1). After purification, relatively few AuNRs are freely dispersed or otherwise not associated with the PS@AuNRs assemblies (Fig. 1), which suggests that the AuNRs assemble efficiently onto the surfaces of the PS spheres.

The average surface coverage of the AuNRs on the PS cores was controlled by tuning the concentration of AuNRs relative to that of the PS spheres dispersed in the ethanol solution during the self-assembly process. We prepared samples with a low surface coverage of 81 ± 5 AuNRs per PS core (Fig. 1a), a medium surface coverage of 307 ± 12 AuNRs per PS core (Fig. 1b), and a high surface coverage of nearly 400 AuNRs (389 ± 21) on each PS core (Fig. 1c). The distance between individual AuNRs within these PS@AuNRs assemblies decreases with an increased surface coverage on the PS as determined from analysis of the TEM results. This increased surface coverage of AuNRs leads to more interactions between the individual AuNRs, and a transition in the orientation of the AuNRs relative to the surfaces of the PS spheres (Fig. 1c-f). The AuNRs

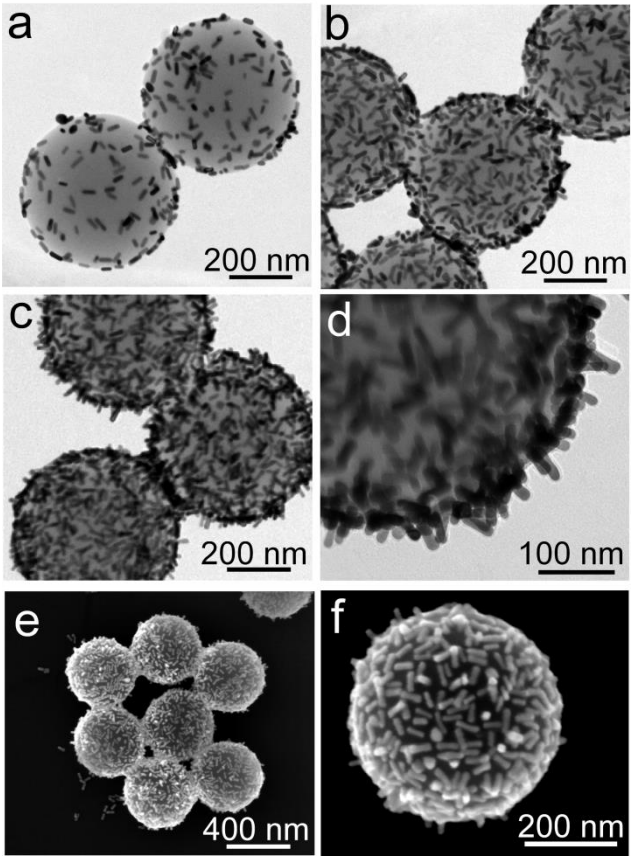

Fig. 1 Tuneable surface loading of gold nanorods (AuNRs) on polystyrene (PS) colloids. (a-c) Transmission electron microscopy (TEM) images of PS colloids with a sequential increase in surface loading of AuNRs, respectively. (d) Higher magnification TEM image depicting the organization of AuNRs on a PS colloid. (e,f) Scanning electron microscopy (SEM) images of PS coated with a high surface loading of AuNRs.

adopt random orientations relative to each other on the surfaces of the PS spheres. Some of the AuNRs appear to have less contact with the PS cores at a high surface loading, and adopt an orientation with their long-axis nearly perpendicular to the surfaces of the PS cores (Fig. 1d). This results in 'spiky' features of AuNRs on the PS sphere surfaces. The evolution in surface topography (from smooth to bumpy to spiked) is most likely due to the favourable interactions between the amine-terminated PS surfaces and the AuNRs and the repulsive interactions (e.g., electrostatic) between neighbouring AuNRs.

The PS@AuNRs assemblies form slowly through specific interactions between the PVP/SDS coated AuNRs and the PS spheres. The slow rate of formation of the PS@AuNRs assemblies (2 days) could be attributed to electrostatic repulsions between neighbouring gold nanorods, as well as the possible rearrangement of PVP and SDS on the surfaces of the AuNRs simultaneous to coordination with the amine-functionalized PS spheres.[25] The PVP/SDS coated AuNRs can be easily dispersed into some aqueous solutions,[27,28] but the PS@AuNRs settle from aqueous solutions after >1 day due to their increased density relative to that of the PS spheres alone. In contrast, an ethanol solution can stabilize the interactions between PVP, SDS, AuNRs, and amine-functionalized PS spheres during and after the assembly process forming a suspension with a milky pink coloration. The specific interactions between the amine-functionalized PS spheres and the PVP and SDS capped AuNRs are further supported by the results of a control experiment using PS spheres functionalized with carboxylic acid groups. A dispersion of PVP/SDS stabilized AuNRs in either ethanol

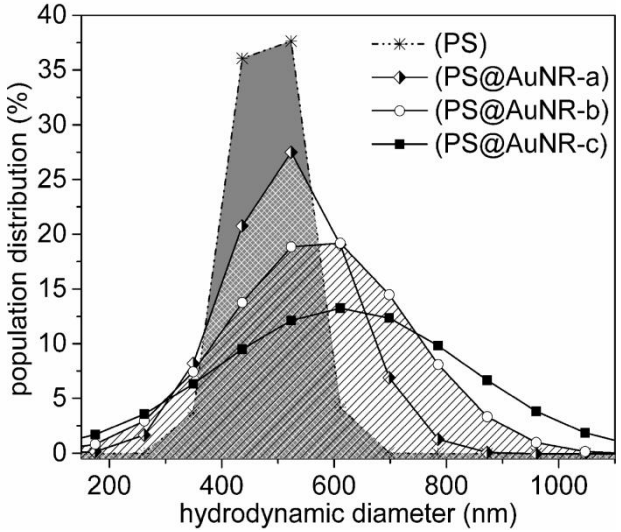

Fig. 2 Characterization of hydrodynamic diameter by dynamic light scattering for PS colloids and three different PS@AuNRs assemblies. An increase in surface loading of AuNRs on PS colloids (low to medium to high loading; or a, b, and c, respectively) results in an increase of the average hydrodynamic diameter of the assemblies.

or acidified ethanol with a suspension of carboxylic acid functionalized PS spheres did not form PS@AuNRs assemblies after 2 days (Fig. S2). The amine-functionality of the PS spheres is, therefore, important to stabilize the PVP/SDS capped AuNRs on the surfaces of these spheres. Assemblies suspended in either water or ethanol had an average surface potential of -30 mV as determined by zeta potential measurements. Similar surface potential values were obtained for the original amine-functionalized PS spheres, as well as for assemblies with different loadings of AuNRs. These results further confirm that the formation of the assemblies does not alter the colloidal stability of the AuNRs or the amine-functionalized PS spheres.

An increase in the surface coverage of AuNRs on the PS cores is correlated with an increase in the measured hydrodynamic diameter of the assemblies. The average hydrodynamic diameter increases from 487 nm for the bare PS core to 509 nm, 557 nm and 586 nm for the low, medium and high surface coverage PS@AuNRs assemblies (Fig. 2), respectively. The dynamic light scattering results indicate that the assemblies form a colloidal suspension without any indication of aggregation. The observed increase in hydrodynamic diameter with increased surface coverage of AuNRs is also accompanied with an increased dispersion in particle size (Fig. 2). This decrease in uniformity of the hydrodynamic size with increased loading of AuNRs is likely the result of an increased surface roughness of the assemblies with the AuNRs forming 'spike' like features that are distributed non-uniformly over the PS cores (Fig. 1). Despite this variation in surface topography and hydrodynamic diameter of the low to high loading of AuNRs, all of these assemblies exhibited a similar colloidal and long-term stability (see Electronic Supplementary Information for further details).

The PS@AuNRs assemblies are simple to prepare and form stable surfaces with attractive optoelectronic properties for use in sensing applications. The combination of the LSPR of the gold nanoparticles and the demonstrated tuneable surface roughness of the assemblies are attractive as a potential substrate for SERS. We evaluated the SERS response of three PS@AuNRs samples with different surface coverage of AuNRs using 1,4-benzenedithiol (1,4-BDT) as the probe molecule (Fig. 3). The loadings of AuNRs per PS core were 43±3, 294±10 and 376±16 for PS@AuNR-1, -2 and -3, respectively. The assemblies with the highest loading of AuNRs (PS@AuNR-3) had ~9 times more AuNRs than the PS@AuNR-1 assemblies, and ~1.3 times more AuNRs than the PS@AuNR-2 assemblies. All samples of PS@AuNRs exhibited SERS activity for 1,4-BDT. The Raman

spectral characteristics of 1,4-BDT has been well documented in the literature and 1,4-BDT is widely used to demonstrate the effect of SERS for a diverse range of nanostructures and nanostructured films.[23,29-31] In our SERS analysis, the PS@AuNRs assemblies were excited at a wavelength of 785 nm. The longitudinal plasmon resonance band is centred at 770 nm for a suspension of individual AuNRs and broadened upon their assembly onto surfaces of the PS cores (Fig. S5 and S6). Overlap between the excitation wavelength of the laser and the longitudinal SPR band of AuNRs was chosen to maximize the amplification of the Raman spectral intensities of 1,4-BDT bound to the AuNRs. The peak position of this SPR band could be further tuned through controlling the aspect ratio of the AuNRs,[32,33] though this is beyond the scope of our study.

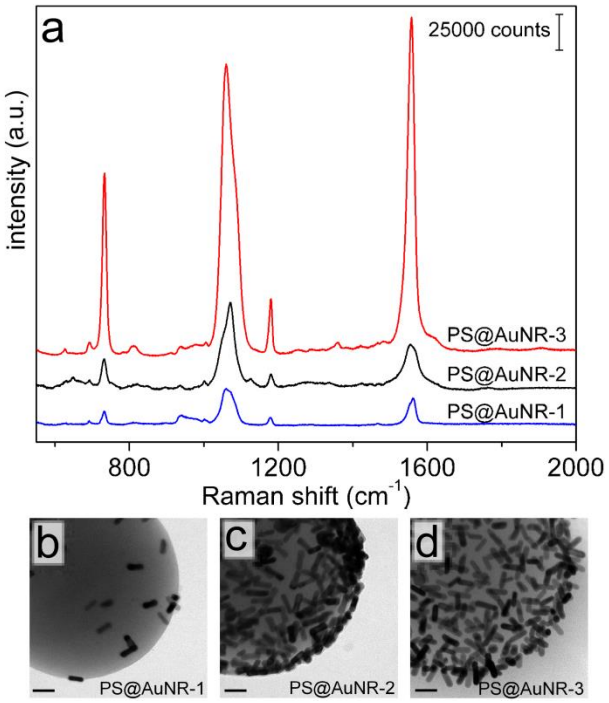

Fig. 3 (a) Surface-enhanced Raman spectra of 1,4-benzenedithiol (1,4-BDT) adsorbed onto three different samples of PS@AuNRs with an increasing loading of AuNRs on the PS core. These samples are referred to as PS@AuNR-1, PS@AuNR-2 and PS@AuNR-3, respectively, as noted above each spectrum. Spectra were obtained using a 785 nm laser (~4.2 mW/μm^2) with an exposure time of 20 s. (b,c,d) Representative TEM images of PS@AuNRs assemblies depicting the three different loadings of AuNRs, respectively. Scale bars in each TEM image are 50 nm in length.

The Raman spectra obtained by SERS analysis differs between the three types of PS@AuNRs assemblies. Four characteristic Raman signals of 1,4-BDT, located at 1557, 1180, 1059 and 732 cm^{-1}, were observed in each spectrum, but differences were observed in their relative intensities. The PS@AuNR-3 assemblies enhanced the Raman signals of 1,4-BDT by at least 10 times on average in comparison to that observed for the PS@AuNR-1 assemblies, and at least 5 times to that measured for the PS@AuNR-2 assemblies. The broad peak at 1059 cm^{-1} was observed in all SERS spectra, which is attributed to the broadening and overlap of two separate ordinary Raman bands in this region (1080 and 1065 cm^{-1}).[34] This phenomenon is indicative of interactions between the surfaces of the AuNRs and the π-orbital system of the 1,4-BDT benzene ring.[29,34] Bridging of the 1,4-BDT molecules between neighbouring AuNRs result in further enhancement of this band due to the close proximity of AuNRs adhered on the surfaces of PS spheres.

Enhancement observed in the Raman spectra appears, upon initial inspection, to scale according to the average number of AuNRs present on the surfaces of the PS (Fig. 3a). Upon further inspection though, the enhancement exhibited by the PS@AuNR-3 assemblies is more than can be accounted for by a simple increase in average number of AuNRs present on the PS cores. These results imply that the surface topography of the AuNRs assembled onto the PS cores might have an impact on the SERS activity of these substrates. This conclusion is further supported through a detailed comparison of the PS@AuNR-2 and PS@AuNR-3 assemblies. The topography of the PS@AuNR-2 assemblies is bumpy with the AuNRs oriented with their length parallel to the surfaces of the PS cores. The PS@AuNR-3 assemblies, on the other hand, contain ~28% more AuNRs and have a much rougher topography with 'spikes' of AuNRs on the surfaces of PS cores. The average distances between neighbouring AuNRs on the PS cores are ~12 nm and ~8 nm on average for PS@AuNR-2 and -3 assemblies, respectively. The SERS activity of PS@AuNR-3 is, however, on average at least 5 times higher than that observed for the PS@AuNR-2 assemblies (Fig. 3a). The roughened surface topography and decreased distance between individual AuNRs in the PS@AuNR-3 assemblies effectively amplify the enhancement of all four characteristic Raman bands of 1,4-BDT. These properties of the PS@AuNR-3 assemblies make it the best substrate among our three samples for SERS through the generation of more hot spots per surface area, which arise from small gaps between individual AuNRs (~5 nm) that establish intense local electric fields.[16] In summary, the PS@AuNRs assemblies can be used as effective SERS substrates and the unique surface topography of these assemblies can further enhance the Raman spectra of molecules bound to the AuNRs. The ability to tune the loading of AuNRs and to alter their surface topography while maintaining their long-term colloidal stability could prove to be useful in a variety of sensing applications.

We demonstrate the preparation of a series of core-shell materials through the self-assembly of gold nanorods onto spherical polystyrene colloidal templates. These assemblies were prepared with a tuneable loading of gold nanorods. The surface coverage or number of adsorbed gold nanorods in these assemblies was varied by approximately one order of magnitude. Of particular interest is a transition from relatively smooth to highly uneven or 'spiky' surfaces prepared by self-assembly nanorods at relatively high loadings of gold nanorods. These assemblies exhibit colloidal stability when dispersed in alcohol based solutions and retain their surface topography and surface coverage of gold nanorods over a period of at least one year when stored in solution or isolated as a powder. The plasmonic properties of the assemblies in combination with the tuneable surface topography of their shell of gold nanorods, might be useful in optical-based sensing applications. The application of these core-shell materials for SERS was demonstrated for assemblies coated with 1,4-benzenedithiol. All of the core-shell assemblies exhibited SERS activities, and the observed enhancement was primarily correlated with an increased surface coverage of gold nanorods on the cores. A further enhancement was, however, observed with the transition in surface topography, roughness and average density of the gold nanorods within the assembled shell. This transition from bumpy to 'spiky' surfaces was associated with a further enhancement of the Raman spectrum of 1,4-benzenedithiol bound to the nanorods that did not correlate only to the increased loading of gold nanoparticles. For example, a relative increase of ~28% loading of gold nanorods led to an enhancement in the Raman spectrum of at least 5 times on average. The colloidal stability, as well as the control over the loading and surface topography, of the gold nanorods assembled onto polystyrene colloids could provide a versatile substrate for SERS based sensing applications. These core-

shell assemblies also form a functional platform for analysing the influence of colloidal particles' surface topography on their observed physicochemical properties.

This work was supported in part by the Natural Sciences and Engineering Research Council (NSERC) of Canada, the Canada Research Chairs Program (B.D. Gates), and the Undergraduate Work-Study Program (I.W. Guo) from Simon Fraser University. This work made use of 4D LABS shared facilities supported by the Canada Foundation for Innovation (CFI), British Columbia Knowledge Development Fund (BCKDF), Western Economic Diversification Canada, and Simon Fraser University.

Notes and references

[a] *Department of Chemistry, Simon Fraser University,*

8888 University Drive, Burnaby, BC V5A 1S6, Canada.

E-mail: bgates@sfu.ca; Fax: +1 778-782-3765; Tel: +1 778-782-8066

†Electronic Supplementary Information (ESI) available: Further experimental details on the preparation and characterization of the PS@AuNRs assemblies, a representative TEM image of the PVP/SDS capped gold nanorods, TEM images from a mixture of PVP/SDS capped gold nanorods and carboxylic acid functionalized PS spheres, TEM data on the stability of PS@AuNRs assemblies at pH 12, details on the stability of these materials when stored over a period of one year, an extinction spectrum for an aqueous dispersion of these nanorods, an extinction spectrum associated with the PS@AuNR assemblies, and further data and analysis for the SERS studies. See DOI: 10.1039/c000000x/

1 R. G. Chaudhuri, S. Paria, *Chem. Rev.*, 2012, **112**, 2373-2433.

2 B. J. Jankiewicz, D. Jamiola, J. Choma, M. Jaroniec, *Adv. Colloid Interface Sci.*, 2012, **170**, 28-47.

3 C. S. Levin, C. Hofmann, T. A. Ali, A. T. Kelly, E. Morosan, P. Nordlander, K. H. Whitemire, N. J. Halas, *ACS Nano*, 2009, **3**, 1379-1388.

4 M. Chen, Y. N. Kim, H. M. Lee, C. Li, S. O. Cho, *J. Phys. Chem. C*, 2008, **112**, 8870-8874.

5 R. Bardhan, N. K. Grady, T. Ali, N. J. Halas, *ACS Nano*, 2010, **4**, 6169-6179.

6 J. McBride, J. Treadway, L. C. Feldman, S. J. Pennycook, S. J. Rosenthal, *Nano Lett.*, 2006, **6**, 1496-1501.

7 J. Zhang, Y. Fu, J. R. Lakowicz, *J. Phys. Chem. C*, 2007, **111**, 1955-1961.

8 S. Xuan, Y.–X. J. Wang, J. C. Yu, K. C.–F. Leung, *Langmuir*, 2009, **25**, 11835-11843.

9 S. W. Kang, Y. W. Lee, Y. Park, B.–S. Choi, J. W. Hong, K.–H. Park, S. W. Han, *ACS Nano*, 2013, **7**, 7945-7955.

10 S.-Y. Chang, L. Liu, S. A. Asher, *J. Am. Chem. Soc.*, 1994, **116**, 6739-6744.

11 Y. Yin, Y. Lu, B. Gates, Y. Xia, *Chem. Mater.*, 2001, **13**, 1146-1148.

12 Z. Zhong, Y. Yin, B. Gates, Y. Xia, *Adv. Mater.*, 2000, **12**, 206-209.

13 H. Kang, S. Jeong, Y. Park, J. Yim, B.–H. Jun, S. Kyeong, J.–K. Yang, G. Kim, S. Hong, L. P. Lee, J.–H. Kim, H.–Y. Lee, D. H. Jeong, Y.–S. Lee, *Adv. Funct. Mater.*, 2013, **23**, 3719-3727.

14. Y. Li, Y. Pan, L. Zhu, Z. Wang, D. Su, G. Xue, *Macromol. Rapid Commun.*, 2011, **32**, 1741.

15 I. Pastoriza-Santos, D. Gomez, J. Perez-Juste, L. M. Liz-Marzan, P. Mulvaney, *Phys. Chem. Chem. Phys.*, 2004, **6**, 5056-5060.

16 B. Sadtler, A. Wei, *Chem. Commun.*, 2002, 1604-1605.

17 S. C. Padmanabhan, J. McGrath, M. Bardosova, M. E. Pemble, *J. Mater. Chem.*, 2012, **22**, 11978-11987.

18 Y. Xia, J. Li, L. Jiang, *J. Coll. Interface Sci.*, 2012, **377**, 34-39.

19 N. Phonthammachai, J. C. Y. Kah, G. Jun, C. J. R. Sheppard, M. C. Olivo, S. G. Mhaisalkar, T. J. White, *Langmuir*, 2008, **24**, 5109-5112.

20 H. Y. Koo, W. S. Choi, D.–Y. Kim, *Small*, 2008, **4**, 742-745.

21 J.–H. Lee, D. O. Kim, G.–S. Song, Y. Lee, S.–B. Jung, J.–D. Nam, *Macromol. Rapid Commun.*, 2007, **28**, 634-640.

22 N. R. Jana, T. Pal, *Adv. Mater.*, 2007, **19**, 1761-1765.

23 K. D. Osberg, M. Rycenga, N. Harris, A. L. Schmucker, M. R. Langille, G. C. Schatz, C. A. Mirkin, *Nano Lett.*, 2012, **12**, 3828-3832.

24 A. M. Gabudean, M. Focsan, S. Astilean, *J. Phys. Chem. C*, 2012, **116**, 12240-12249.

25 M. Behera, S. Ram, *Appl. Nanosci.*, 2013, **4**, 247-254.

26 N. G. Greeneltch, M. G. Blaber, A.–I. Henry, G. C. Schartz, R. P. Van Duyne, *Anal. Chem.*, 2013, **85**, 2297-2303.

27 I. C. Pekcevik, L. C.H. Poon, M. C.P. Wang, B. D. Gates, *Anal. Chem.*, 2013, **85**, 9960-9967.

28 S. K. Seol, D. Kim, S. Jung, W. S. Chang, Y. M. Bae, K. H. Lee, Y. Hwu, *Mater. Chem. Phys.*, 2012, **137**, 135-139.

29 S. H. Cho, H. S. Han, D.-J. Jang, K. Kim, M. S. Kim, *J. Phys. Chem.*, 1995, **99**, 10594-10599.

30 S. W. Joo, S. W. Han, K. Kim, *J. Coll. Inter. Sci.*, 2001, **240**, 391-399.

31 M. Rycenga, P. H. C. Camargo, W. Li, C. H. Moran, Y. Xia, *J. Phys. Chem. Lett.*, 2010, **1**, 696-703.

32 C. J. Murphy, N. R. Jana, *Adv. Mater.*, 2002, **14**, 80-82.

33 B. Nikoobakht, M. A. El-Sayed, *Chem. Mater.*, 2003, **15**, 1957-1962.

34 Q. Zhang, W. Li, C. Moran, J. Zeng, J. Chen, L.-P. Wen, Y. Xia, *J. Am. Chem. Soc.*, 2010, **132**, 11372-11378.